

## Giant Bulk Photovoltaic Effect under Linearly Polarized X-Ray Synchrotron Radiation

G. Dalba and Y. Soldo

*Dipartimento di Fisica dell'Università degli Studi di Trento, I-38050 Povo (Trento), Italy*

F. Rocca

*Centro Consiglio Nazionale delle Ricerche di Fisica degli Stati Aggregati, I-38050 Povo (Trento), Italy*

V. M. Fridkin

*Institute of Crystallography of the Russian Academy of Sciences, 117333 Moscow, Russia*

Ph. Saintavit

*Laboratoire de Minéralogie-Cristallographie, CNRS URA 9, Université Paris 6 & 7,*

*4 place Jussieu, 75252 Paris Cedex 05, France*

(Received 10 August 1994)

The angular dependencies of the linear bulk photovoltaic effect (BPE) under linearly polarized x-ray synchrotron radiation in  $\text{LiNbO}_3\text{:Fe}$ ,  $\text{La}_3\text{Ga}_5\text{SiO}_{14}\text{:Pr}$ , and  $\text{SiO}_2$  have been revealed. This is the first observation of the tensorial properties of BPE under polarized x rays, which reveals giant values of the components of the photovoltaic tensor  $G_{ijk}$ . The values of  $G_{ijk}$  at 850 eV are 3–6 orders of magnitude higher than the corresponding values for the optical region. The present results may also explain the origin of x-ray photorefractive effect previously observed in  $\text{LiNbO}_3\text{:Fe}$ .

PACS numbers: 72.40.+w

The bulk photovoltaic effect (BPE) in crystals without center of symmetry has been widely investigated in the optical spectral region [1,2]. The BPE consists of the creation of a steady state photocurrent at uniform illumination of homogeneous crystals without center of symmetry. It is shown that BPE is connected with the violation of the principle of detailed balancing for the nonequilibrium carriers in piezoelectric and ferroelectric crystals. This violation, in turn, is connected with two possible mechanisms, ballistic and shift [2]. The ballistic mechanism is connected with the asymmetric part of the distribution function of the nonequilibrium carriers. In this case BPE is caused by the asymmetry of the generation, recombination, or scattering of nonequilibrium carriers, excited by the light. The BPE is due to nonthermalized electrons, which contribute to the bulk photovoltaic current only during the relaxation time. The shift mechanism is connected with the shift of the photoexcited carriers in the real space of the lattice.

The BPE in  $\text{LiNbO}_3$  in the x-ray region was qualitatively observed earlier [3,4], but neither tensorial properties nor the values of the photovoltaic tensor components were obtained. The measurements presented in this Letter were performed for the ferroelectric crystal  $\text{LiNbO}_3\text{:Fe}$  (point group  $3m$ ) and the piezoelectric crystal  $\text{La}_3\text{Ga}_5\text{SiO}_{14}\text{:Pr}$  and  $\text{SiO}_2$  (naturally colored and synthetic quartz) which belong to the point group  $3:2$ . The BPE in the optical region was investigated in these crystals earlier [1,2,5]. The sample of  $\text{LiNbO}_3$  was doped with Fe atoms with concentration approximately equal to  $10^{19} \text{ cm}^{-3}$ ; it was oriented along the  $x$ ,  $y$ , and  $z$  directions ( $x \parallel m$ ,  $z \parallel 3$ , respectively), and had dimen-

sions  $4 \times 3 \times 3 \text{ mm}^3$ . The crystal of  $\text{La}_3\text{Ga}_5\text{SiO}_{14}\text{:Pr}$ , doped with  $\text{Pr}^{3+}$  ions with concentration approximately equal to  $3.5 \times 10^{20} \text{ cm}^{-3}$ , was oriented along  $x$ ,  $y$ ,  $z$  directions ( $x \parallel 2$ ,  $z \parallel 3$ , respectively) and had dimensions  $5 \times 4 \times 3 \text{ mm}^3$ . The piezoelectric crystal of synthetic and natural quartz, with size  $5 \times 5 \times 1 \text{ mm}^3$ , had the same orientation. The schematic representation of the experiment is shown in Figs. 1(a) and 1(b).

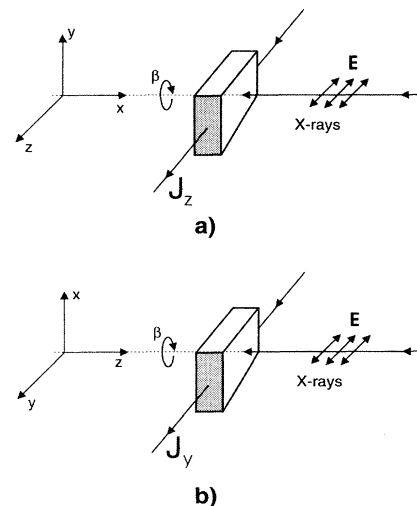


FIG. 1. Geometry of the BPE measurements in  $\text{LiNbO}_3\text{:Fe}$  (a) and in  $\text{La}_3\text{Ga}_5\text{SiO}_{14}\text{:Pr}$  (b).  $\mathbf{E}$  is the polarization axis of the x-ray beam,  $J_z$  or  $J_y$  is the bulk photovoltaic current along appropriate axis for the crystal under study, and  $\beta$  is the angle between the x-ray polarization and the photovoltaic current.

The measurements were carried out at the storage-ring SuperACO of LURE (Laboratoire pour l'Utilisation du Rayonnement Electromagnetique), Orsay, France. The photons, delivered by the asymmetric wiggler inserted on the straight section SU2, were monochromatized by a two crystal beryl monochromator; the bandwidth was equal to 0.28 eV. The linear polarization was superior to 99.9%. For photons emitted in the orbital plane, the calculated flux on a  $3 \times 3 \text{ mm}^2$  sample at 850 eV was  $1.24 \times 10^7$  photons per second for a 400 mA machine current. The crystals were mounted in a vacuum chamber, at a pressure less than  $10^{-6}$  mbar, on a linear  $x, y, z$  translator with a rotation device which adjusted the angle  $\beta$  between the x-ray polarization plane and the current-carrying crystal axis. The photovoltaic current was collected by a picoammeter with a sensitivity of 10 fA (Keithley 486). Data were digitally stored and averaged; the x-ray beam intensity before the sample was also detected.

The linear BPE is described by the third-rank tensor  $G_{ijk}$  (Glass coefficient), analogous to the piezoelectric one [2]; the components  $J_i$  of the photovoltaic current are related to  $G_{ijk}$  by the relationship

$$J_i = \frac{1}{2} \alpha G_{ijk} (E_j E_k^* + E_j^* E_k), \quad (1)$$

where  $\alpha$  is the absorption coefficient, and  $E_j$  and  $E_k$  are projections of the incident beam polarization vector. In Eq. (1) we suppose that absorption anisotropy is unimportant. Taking into account nonzero components of the  $G_{ijk}$  tensor for the trigonal point group  $3m$ , to which the ferroelectric  $\text{LiNbO}_3$  belongs, we obtain, from Eq. (1), the expression for current  $J_z$  in the case of linearly polarized beam propagation along  $x$  axis,

$$J_z^0 = \alpha G_{31} I + \alpha (G_{33} - G_{31}) I \cos^2 \beta. \quad (2)$$

Here  $I$  is the intensity of the beam and  $\beta$  is the angle between the beam polarization vector and the  $z$  axis [see Fig. 1(a)]. In Eq. (2) the abbreviated subscript notation is used, i.e.,  $G_{ijk} = G_{i\mu}$ , where  $\mu = 1, \dots, 6$  represents the six distinct values of the pair  $j, k$  [2].

For point group 3:2, to which the piezoelectric crystals of  $\text{La}_3\text{Ga}_5\text{SiO}_{14}$  and quartz belong, the dependence of current  $J_y$  on the angle  $\beta$  in the case of linearly polarized beam propagation along the  $z$  axis has the form

$$J_y^0 = \alpha G_{11} I \sin 2\beta, \quad (3)$$

where  $\beta$  is the angle between beam polarization vector and the  $x$  axis [see Fig. 1(b)]. In Eqs. (2) and (3)  $J_z^0$  and  $J_y^0$  are the current densities which flow in the surface layer of the crystal face in which the incident x-ray beam is absorbed with penetration depth  $\alpha^{-1}$ . The experimental results are shown in Figs. 2 and 3. Figure 2 shows the time dependence of the bulk photovoltaic current in  $\text{LiNbO}_3:\text{Fe}$ ; the switching time of the synchrotron beam is shown by arrows. The photovoltaic current decay in Fig. 2 is mainly due to the decrease of the x-ray beam

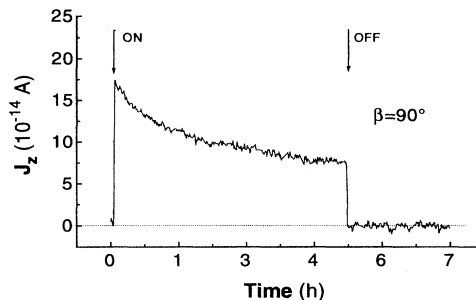


FIG. 2. Time dependence of the bulk photovoltaic current  $J_z$  in  $\text{LiNbO}_3:\text{Fe}$ ,  $\beta = 90^\circ$ .

intensity and partially to the pyroelectric effect. By investigating the angular dependencies, only the stationary values of current were taken into account. The experimental angular dependencies  $J = J(\beta)$  are shown in Fig. 3. Figure 3(a) (circles) shows the angular dependence of  $J_z = J_z(\beta)$  in  $\text{LiNbO}_3:\text{Fe}$ , which coincides with Eq. (2) for  $G_{31} \approx 0.6 \times 10^{-6} \text{ cm V}^{-1}$  and  $G_{33} \approx 3 \times 10^{-6} \text{ cm V}^{-1}$ . Figure 3(b) (squares) shows the angular dependence of  $J_y = J_y(\beta)$  in  $\text{La}_3\text{Ga}_5\text{SiO}_{14}:\text{Pr}$ , which coincides with Eq. (3) for  $G_{11} \approx 2.5 \times 10^{-7} \text{ cm V}^{-1}$ . The error bars in Fig. 3 take into account the current changes due to crystal tilt during rotation.

Table I shows the comparison of the photovoltaic tensor components for the optical and x-ray regions. In all the investigated crystals the linear BPE in the optical region is caused mainly by the ballistic mechanism and by the asymmetric optical excitation of the impurity

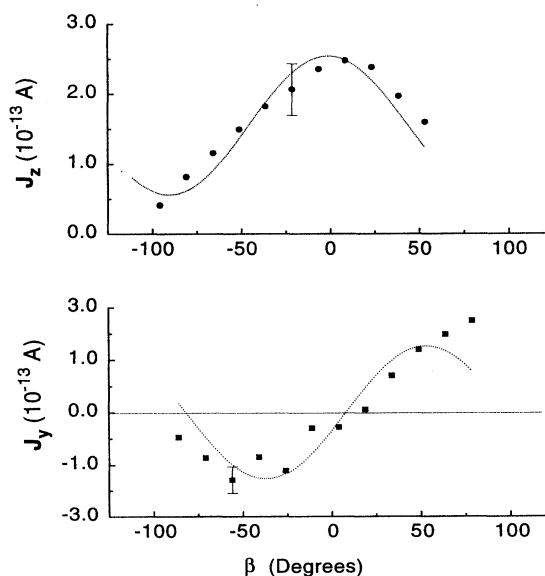


FIG. 3. Angular dependence of the bulk photovoltaic currents  $J_z$  in  $\text{LiNbO}_3:\text{Fe}$  (circles) and  $J_y$  in  $\text{La}_3\text{Ga}_5\text{SiO}_{14}:\text{Pr}$  (squares); theoretical curves (dotted lines).

TABLE I. Glass coefficients for  $\text{LiNbO}_3\text{:Fe}$ ,  $\text{La}_3\text{Ga}_5\text{SiO}_{14}\text{:Pr}$ , and quartz for optical and x-ray regions.

	Optical region			X-ray region		
	$\lambda$ (nm)	$\alpha$ ( $\text{cm}^{-1}$ )	$G_{ijk}$ ( $\text{cm V}^{-1}$ )	$\lambda$ ( $\text{\AA}$ )	$\alpha$ ( $\text{cm}^{-1}$ )	$G_{ijk}$ ( $\text{cm V}^{-1}$ )
$\text{LiNbO}_3\text{:Fe}$	514.5	5	$G_{31} \approx 2 \times 10^{-9}$ $G_{33} \approx 4 \times 10^{-9}$ [2]	15.5	$3 \times 10^4$ [6]	$G_{31} \approx 6 \times 10^{-7}$ $G_{33} \approx 3 \times 10^{-6}$
$\text{La}_3\text{Ga}_5\text{SiO}_{14}\text{:Pr}$	514.5	0.45	$G_{11} \approx 2 \times 10^{-11}$ [5]	15.5	$1.8 \times 10^4$ [6]	$G_{11} \approx 2.5 \times 10^{-7}$
$\text{SiO}_2$ natural	300–500	2	$G_{11} \approx 3 \times 10^{-13}$ [2]	15.5	$1.0 \times 10^4$ [6]	$G_{11} \approx 4 \times 10^{-7}$
$\text{SiO}_2$ synthetic	300–500	< 0.05	$G_{11} < 3 \times 10^{-14}$ [2]	15.5	$1.0 \times 10^4$ [6]	$G_{11} \approx 4 \times 10^{-7}$

centers:  $\text{Fe}^{+2}$  in  $\text{LiNbO}_3\text{:Fe}$ ,  $\text{Pr}^{+3}$  in  $\text{La}_3\text{Ga}_5\text{SiO}_{14}\text{:Pr}$ , and  $F$  centers in the naturally colored quartz [1,2,5]. For the synthetic quartz in the optical region there is no BPE at all [2]. It is seen from Table I that  $G_{ijk}$  for x-ray energy 850 eV is 3–6 orders of magnitude higher than the corresponding tensor components for the optical region. The BPE in the x-ray region is not connected with impurity centers. For example, there is no difference in  $G_{11}$  for the naturally colored and synthetic crystals of quartz. This first observation of the tensorial properties of the bulk photovoltaic current under polarized synchrotron beam definitively confirms the existence of the x-ray BPE.

Giant values of Glass coefficients  $G_{ijk}$  lead, in turn, to giant values of the free path of the nonthermalized carriers excited by x rays. For example, if we consider ballistic mechanism of BPE caused by the asymmetric photoexcitation of carriers, the Glass coefficient is given by [2]

$$G = e l_0 \Phi \xi^{\text{ex}} (\hbar \omega)^{-1}, \quad (4)$$

where  $l_0$  is the mean free path,  $\hbar \omega$  is the photon energy,  $\Phi$  is the quantum yield, and  $\xi^{\text{ex}}$  is the photoexcitation asymmetry parameter. Model formulas suggest that, for optical energies [2],

$$\xi_{\text{max}}^{\text{ex}} \leq 10^{-1} - 10^{-2}.$$

For  $\text{LiNbO}_3\text{:Fe}$ , in the optical range, it gives  $l_0 \approx 10^2 - 10^3 \text{ \AA}$ . The substitution of  $G \approx 10^{-6} \text{ cm V}^{-1}$ , which was obtained for  $\text{LiNbO}_3\text{:Fe}$  in the x-ray region ( $\hbar \omega = 850 \text{ eV}$ ), in Eq. (4) gives

$$l_0 \approx 10^5 (\xi^{\text{ex}})^{-1} \text{ \AA}.$$

If we assume that  $\xi^{\text{ex}} < 1$  and that the quantum yield  $\Phi$  is equal to 1 as in the visible region, the free path of the nonthermalized carriers  $l_0$  will exceed  $10 \text{ \mu m}$ .

The bulk photovoltaic current  $J_i$  at opened circuit conditions leads to the creation of a static field  $E_i$  [2]:

$$E_i = \frac{J_i}{\sigma_{\text{ph}}} = \frac{\xi^{\text{ex}} l_0}{\mu \tau}, \quad (5)$$

where  $\sigma_{\text{ph}}$  is the total conductivity, and  $\mu$  and  $\tau$  are, respectively, the mobility and the lifetime of the nonequilibrium thermalized carriers. In  $\text{LiNbO}_3\text{:Fe}$  in the optical region  $E_z \approx 10^5 \text{ V cm}^{-1}$ . This strong field connected with low photoconductivity  $\sigma_{\text{ph}}$  leads to the change of birefringence due to the linear electro-optic effect: It was called photorefractive effect and is widely used for the real time holography [7]. Our data show that, in the x-ray region, in  $\text{LiNbO}_3\text{:Fe}$  the field  $E_z$  is very small ( $E_z \leq 1 \text{ V cm}^{-1}$ ) due to the high photoconductivity  $\sigma_{\text{ph}}$ ; this result is also confirmed by previous studies [3]. Nevertheless, the x-ray photorefractive effect was observed in  $\text{LiNbO}_3$ , implying that a large field  $E_z$  much greater than  $1 \text{ V cm}^{-1}$  is present. Moreover, it has been shown that the x-ray photorefractive effect has the same electro-optic

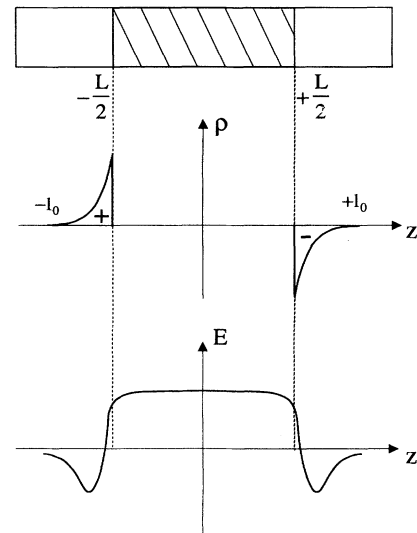


FIG. 4. X-ray photorefractive effect in  $\text{LiNbO}_3\text{:Fe}$  at high values of  $l_0$ . The distribution of the volume charge  $\rho$  and electric field  $E$  after x-ray exposure of the stripe with width  $L$  on the face (100) of the crystal.

nature and is caused by the creation of an electric field [8,9]. It seems that the large mean free path  $l_0 > 10 \mu\text{m}$  obtained from our results explains this apparent contradiction. Figure 4 shows schematically the x-ray exposure of the stripe with width  $L$  on the (100) face of the  $\text{LiNbO}_3\text{:Fe}$  crystal. If we assume that the mean free path of the nonthermalized carriers is larger than the x-ray scattering range, we obtain the electric field in  $z$  direction. This field is caused by the electrons and holes trapped in the *dark* boundary layers with  $l_0$  width. The distribution of the field in the  $z$  direction is shown schematically in Fig. 4 (we consider the bipolar photovoltaic current); it means that the large values of  $l_0$  change the boundary conditions, and so the formula (5) is not valid. This fact must be taken into account at the formation of photorefractive gratings in analogy with photorefractive materials such as bismuth silicate, which have diffusion lengths larger than the grating spacing [7].

- [1] A. M. Glass, D. von der Linde, and T. J. Negran, *Appl. Phys. Lett.* **25**, 233 (1974).
- [2] B. Sturman and V. Fridkin, *The Photovoltaic and Photorefractive Effects in Noncentrosymmetric Materials* (Gordon and Breach Sciences Publishers, Philadelphia, 1992).
- [3] O. F. Schirmer, *J. Appl. Phys.* **50**, 3404 (1979).
- [4] V. M. Fridkin, G. Dalba, P. Fornasini, Y. Soldo, F. Rocca, and E. Burattini, *Ferroelectrics Lett.* **16**, 1 (1993).
- [5] V. M. Fridkin, A. A. Kaminski, V. G. Lazarev, S. B. Astafiev, and A. V. Butashin, *Appl. Phys. Lett.* **55**, 545 (1989).
- [6] B. L. Henke, P. Lee, T. J. Tanaka, R. L. Shimabukuro, and B. K. Fujikawa, *At. Data Nucl. Data Tables* **27**, 1 (1982).
- [7] *Photorefractive Materials and Their Applications*, edited by P. Günter and J. P. Huignard (Springer, Berlin, 1988), Vols. I and II.
- [8] H. Bernhardt, *Phys. Status Solidi (a)* **54**, 597 (1979).
- [9] T. R. Volk, S. A. Shramchenko, and L. A. Shuvalov, *Ferroelectric Lett.* **2**, 55 (1984).